5-2016

Regulation of the reaction between Cytochrome c and Cytochrome Oxidase

Jennifer Silva-Nash

Regulation of the reaction between Cytochrome c and Cytochrome Oxidase

An Honors Thesis submitted in partial fulfillment of the requirements of
Honors Studies in Biochemistry

By
Jennifer Silva-Nash

Spring 2016
Chemistry and Biochemistry
J. William Fulbright College of Arts and Sciences
The University of Arkansas

Acknowledgements

The research in this thesis was sponsored by the Department of Chemistry and Biochemistry at the University of Arkansas, Fayetteville, under the direction of Dr. Frank Millett. The project was funded by an Honors College Research Grant and NIH grants GM20488 and 8P30GM103450. Special thanks go to Marti Scharlau and Dr. Frank Millett for their guidance with the research.

Table of Contents

Abstract

Irreversible brain damage is commonly seen in patients that have suffered strokes, cardiac arrest, or other brain ischemia events. The hypoxic conditions result in neuron death, and previous studies have shown that additional damage occurs when blood flow is restored. It is thought that the lack of energy production during post-ischemia events also causes severe brain damage, as the brain heavily depends on oxidative phosphorylation. Cytochrome c (Cyt *c*) plays a crucial role in this energy production by means of the electron transport chain (ETC), transferring electrons between complexes III (cytochrome bc_1) and IV (cytochrome c oxidase, CcO). Mitochondrial release of Cyt *c* into the cytosol results in type II apoptosis, and release within the mitochondria results in reduction by superoxides, suggesting that Cyt *c* detoxifies reactive oxygen species (ROS). It is also understood that phosphorylation of proteins within the ETC serves a regulation mechanism. We sought to determine whether the phosphorylation of a specific tyrosine (Y) residue within Cyt *c*, Y97, affects the binding kinetics between Cyt *c* and CcO, thus regulating the physiological role of Cyt *c*. We hypothesized that comparison of binding kinetics of mutated Y97E Cyt *c* and wild type Cyt *c*, both to CcO, in an *in vitro* study would reveal insight on the effects of phosphorylation at this specific residue. The Y97 residue was replaced by a glutamate (E) residue– the negative charge from E resembled the negative charge of the phosphate group in phosphorylated Cyt *c*. Both mutant, Y97E, and wild-type, Y97, were synthesized and purified, then subjected to analytical ultracentrifuge and laser photolysis in order to examine the binding kinetics. Results from both analytical ultracentrifuge and laser photolysis revealed little difference in binding between the mutant and the wild-type Cyt *c*.

Introduction and Specific Aims

Oxidative phosphorylation produces 15 times more adenosine triphosphate (ATP) than produced by anaerobic glycolysis. ATP is the primary energy currency of the cell (1) and the process by which ATP is generated through oxidative phosphorylation consists of the electron transport chain (ETC) and ATP synthase. The electron transport chain, found in the inner mitochondrial membrane, is composed of four complexes and two electron carriers: NADH dehydrogenase (complex I), succinate dehydrogenase (complex II), ubiquinone, bc-1 complex (complex III), cytochrome c (Cyt *c*), and cytochrome c oxidase (complex IV) (2). Most electrons enter the ETC via complex I from NADH, which is generated at earlier stages of metabolic processes (glycolysis and the citric acid cycle). Complex II is directly connected to the citric acid cycle and is the only complex that does not pump protons from the mitochondrial matrix to the intermembrane space. The movement of protons generates an electrochemical gradient, which is utilized by ATP synthase (complex V). ATP synthase is a large protein complex, which synthesizes ATP from adenosine diphosphate (ADP) and phosphate by the potential created from the movement of protons.

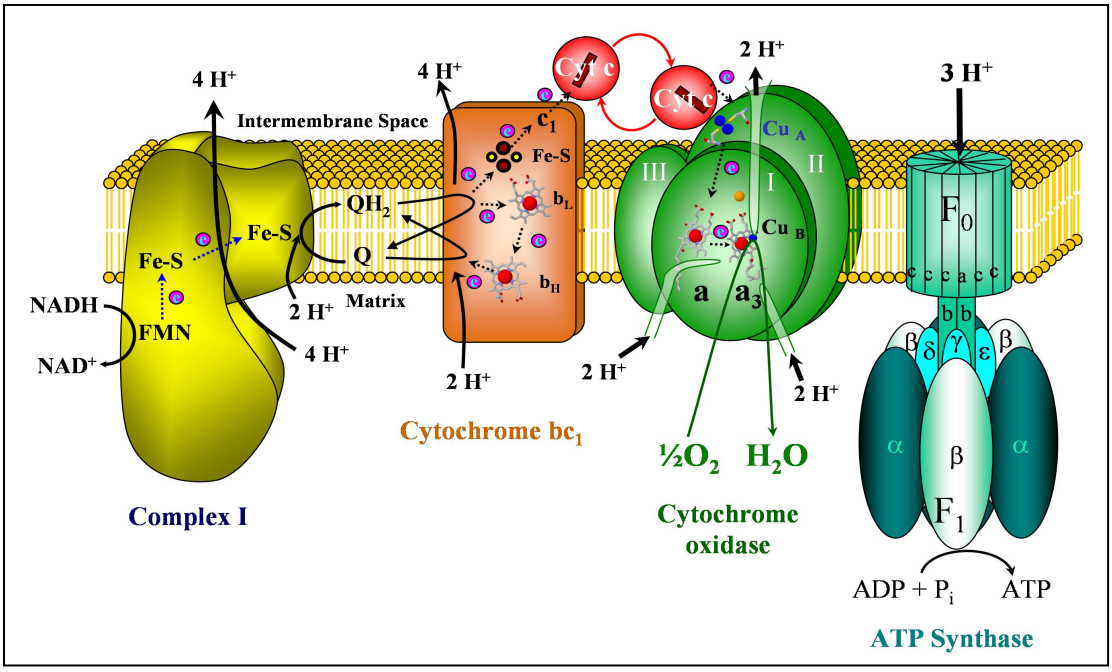

Figure 1. Scheme of the Mitochondrial Electron Transport Chain and Oxidative Phosphorylation

As ATP is a necessary macromolecule for the proper functioning of many organisms, Cyt *c* is a crucial multifunctioning protein. It has a molecular weight of approximately 12,000 Daltons and is composed of 104 amino acids, with a covalently bound protoporphyrin IX heme group. Mammalian Cyt *c* has two major functions: transfer electrons from complex III to complex IVwithin the ETC, and contribution in initiating type 2 apoptosis. Cyt *c* accepts one electron from complex III and transports it to complex IV; this reaction enables the reduction of oxygen into water and the production of ATP. The globular protein is one of the most positively charged proteins (5). A high number of lysine residues on the globular protein surface facilitate interactions with both complexes through electrostatic interactions. These interactions have been proven essential in mice after midgestation, as experimentation revealed that mortality follows this developmental stage in Cyt *c* knockout mice. Studies with

cultured rat embryos assisted in explaining the finding above- energy production relied 5% on aerobic metabolism before gestation day 9 but increased to 95% after gestation day 11 (3).

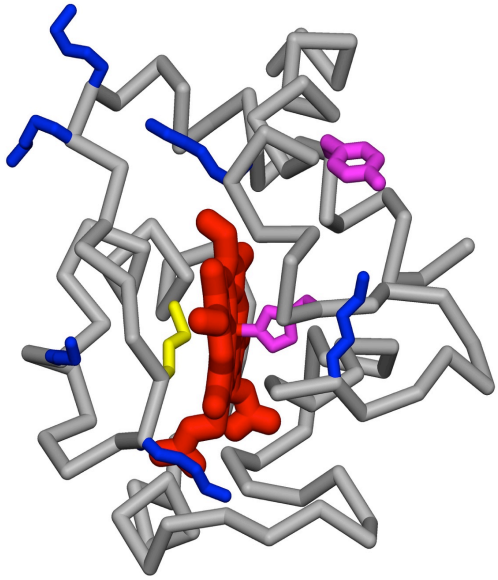

Figure 2: Human Cytochrome C. Tyrosine 97 is in violet

Changes of mitochondrial integrity are accompanied with the release of Cyt *c* into the cytosol, which leads to the initiation of type 2 apoptosis (11). Procaspase-9 is activated to caspase-9 via an apoptosome in a mechanism that is not fully understood, but it is considered that Cyt *c* is an important proapoptotic signal. The sequence of events that occur in cell death as a result of the release of Cyt *c* are speculated to be: change of respiratory rates, reactive oxygen species production, release of Cyt *c* from the mitochondria, apoptosome establishment, and the final caspase activation which triggers apoptosis (2).

Cyt *c* has an additional role within the mitochondria, as it participates in another reduction-oxidation reaction as a reactive oxygen species (ROS) detoxifying enzyme (4, 18). Although oxidative phosphorylation is heavily regulated, mitochondria have been shown to

form variable amounts of ROS, producing oxidative stress to the cell. When Cyt *c* is detached from the mitochondrial membrane, it can be reduced by ROS (5). ROS are potentially damaging molecules, such as peroxide, superoxide, and hydroxide radical. Aging and multiple degenerative diseases have been related to persistent oxidative stress, as both high and low levels ROS result in damage of healthy cells (6). Diseases in which oxidative stress has been implicated include multiple sclerosis, diabetes, glaucoma, ischemic-reperfusion injury, cardiovascular diseases, rheumatoid arthritis, Alzheimer's disease, Parkinson's disease, and mitochondrial diseases (6).

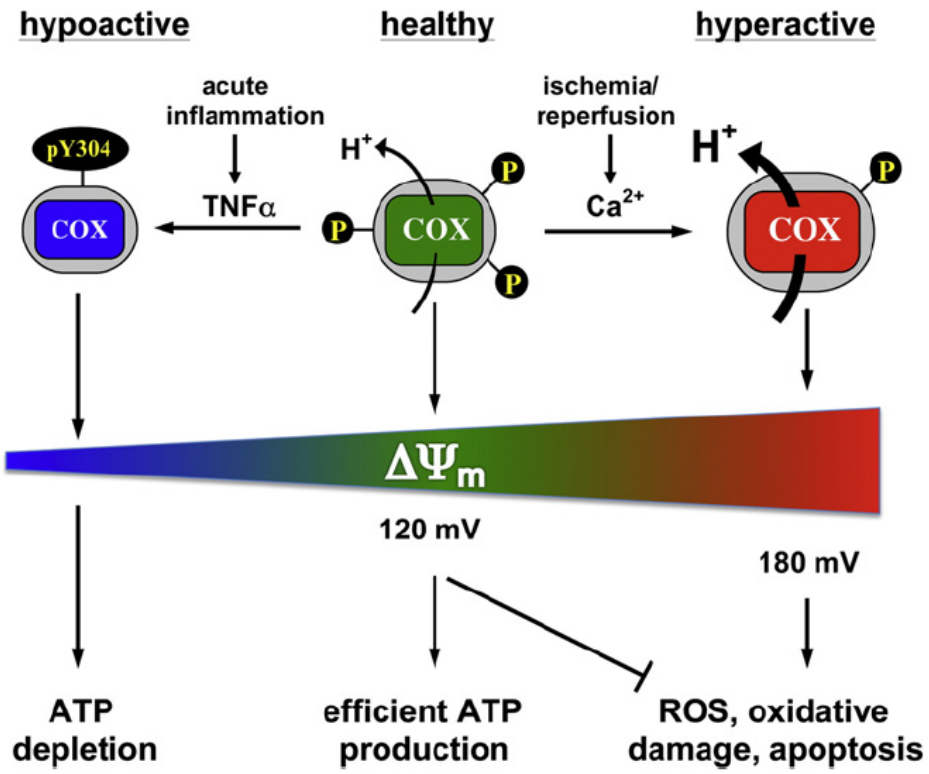

Figure 3: ROS damage is more likely in hyperactive COX (Maik Huttemann et al. Biochimica et Biophysica Acta 1817 (2012) 598–609)

Additionally, reversible brain damage is commonly seen in patients that have suffered strokes, cardiac arrest, or other brain ischemia events. The hypoxic conditions result in neuron death and it is thought that the lack of energy production during post-ischemia events also causes severe brain damage, as the brain heavily depends on oxidative phosphorylation. However, previous studies have shown that additional damage occurs when blood flow is restored. This damage, termed reperfusion injury, results from reestablishment of cellular energy levels. Following an ischemic starvation phase, mitochondria are rapidly restored within five minutes but this hyperactive state results in the overproduction of ROS. As stated above, ROS can trigger apoptosis and can lead to initiation of the ETC and secondary energy failure (2).

There are two roles that Cyt *c* has in ischemia and reperfusion, the loss of Cyt *c* function, thus resulting in secondary energy failure, and initiation of type 2 apoptosis and cell death by the release of Cyt *c* from the mitochondria. (2) The identification of multiple phosphorylation sites have lead to the understanding that the phosphorylation of Cyt *c* is reversible and functions as a regulation mechanism, leading to strong enzyme regulation (2, 4). It has been found that healthy cells contain phosphorylated Cyt *c* proteins. In fact, isolated Cyt *c* from ischemic brain were not phosphorylated and could bind to Apaf1 to initiate downstream caspase activation. (7) It is possible that phosphorylation can regulate the interaction between Cyt *c* and CcO to further serve as a therapeutic intervention to control the amount of damage caused by ischemia/reperfusion. (2)

With the guidance of Dr. Francis Millett, this project studied the binding interactions of Cyt *c* within the ETC. We sought to determine whether the phosphorylation of a specific tyrosine (Y) residue in Cyt *c*, Y97, affects the binding kinetics between Cyt *c* and CcO,

implying a regulation site for the physiologic role of Cyt *c*. We hypothesized that the comparison of binding kinetics of mutated Y97E Cyt *c* and wild type Cyt *c*, both to CcO, in an *in vitro* study would result in understanding the effects of phosphorylation at this specific residue. The Y97 residue was replaced by a glutamate (E) residue– the negative charge from E resembled the negative charge of the phosphate group in phosphorylated Cyt *c*. Both mutant, Y97E, and wild-type, Y97, were synthesized and purified, then subjected to analytical ultracentrifuge and laser photolysis in order to examine the binding kinetics.

Methods

Site-Directed Mutagenesis

Site-directed mutagenesis was required to obtain plasmids with the desired Cyt *c* mutant sequence, Y97E. This process allows for the sequence of the selected recombinant human Cyt *c* plasmid to be altered by insertion, deletion, or substitution.

A Stratagene Quik-Change II site-directed mutagenesis was selected to be used for this procedure. The tyrosine at position 97 of the wild-type Cyt *c*, encoded by TAC, was changed to a nucleotide sequence of GAG. This codon refers to the amino acid glutamate, thus forming the Y97E phosphomimetic sequence. Y97E mutant oligonucleotide sense and antisense primers were ordered from Integrated DNA Technologies, Inc.

Wild-type	5' GCG GAC CTG ATC GCG TAC CTG AAA AAG GCG ACG 3'
Y97E sense primer	5' GCG GAC CTG ATC GCG *GAG* CTG AAA AAG GCG ACG 3'
Y97E antisense primer	5' CGT CGC CTT TTT CAG CTC CGC GAT CAG GTC CGC 3'

Table 1: Wild-type plasmid and sense and antisense primer sequences. Mutated tyrosine codon is underlined in the wild-type sequence, and the corresponding glutamate codon is underlined and italicized in each primer sequence.

Upon the arrival of the designed primers, they were placed within a pulse- centrifuge (VWR Scientific Model V micro centrifuge) for approximately ten seconds and were

suspended in 0.8 mL of sterile, deionized and distilled H_2O (ddi). These samples were incubated at room temperature for approximately two hours. The primers were placed in a -20°C freezer until they were ready to be used.

The primers were allowed to thaw on ice, and a Hewlett- Packard 8452 A Diode Array Spectrophotometer was used to determine the concentration of each primer. This measurement required that 5 μL of each primer be placed in it's respective eppendorf tube, followed by an addition of 495 μL ddi H_2O to each sample. The absorbance readings were taken at 260 nm, the peak absorbance for DNA bases. Taking Beer's Law into account, the absorption reading was equal to the extinction coefficient, the length of the cuvette, and the concentration.

Equation 1: $A=\varepsilon cl$

An extinction coefficient 33 mg mL^{-1} for single-stranded DNA was used and the resulting value for concentration required multiplication by 100, as the dilution was 1:100. With 200 μL as the total volume, each stock primer was diluted to 63 μg $mL^{-1.}$

Proceeding site-directed mutagenesis, reaction mixtures were made from this final dilute stock. Polymerase chain reaction (PCR) technology was used to amplify the number of copies of the mutant plasmid. Thin-walled PCR tubes held 50 μL in volume although the mass of plasmid contained in each tube varied. The amounts of mutagenesis reagents used are indicated in Table 2. Tubes were placed in the thermal cycler and PCR was run according to a preset PCR cycling program, Davis preset, which lasted 2 hours and 45 minutes.

Reaction Tube	A	B
[Parent plasmid], ng/mL	25	12.5
Plasmid, µL	28.8	14
Sense primer, µL	6	6
Antisense primer, µL	6	6
10X Pfu reaction buffer, µL	5	5
dNTP mix, µL	1	1
Pfu polymerase, µL	1	1
Sterile H_2O, µL	2.2	17

Table 2: Y97E Cyt *c* plasmid preparation.

Tubes were taken out of the thermal cycler and allowed to cool on ice to reach a temperature at or below 37 °C. After they have cooled, 1 µL Dpn1 restriction enzyme was added to the tubes to digest the parent enzyme and then incubated for an hour at 37 °C. 5 µL of the Dpn1- DNA mixture was inserted into a pre-chilled Falcon 2054 polypropylene tube. After Epicurian Coli XL-1 Blue supercompetent cells were thawed on ice, 50 µL were added to the treated cells and gently mixed. This mixture was incubated on ice for 30 minutes, and heat-pulsed at 42 °C for 1 minute. An additional 2 minute incubation on ice followed. 0.5 mL of NZY+ broth was added to each tube, and the tubes were incubated at 37 °C for 1 hour with shaking (225-250 rpm). The cell mixtures from each tube were spread over a plate surface, an LB agar plate containing ampicillin (AMP) antibiotic. AMP on the agar plates ensured that only cells with the desired plasmid would be able grow since the Cyt *c* plasmid was engineered to contain a gene for AMP resistance. Plates were placed in an incubator set at 37 °C for 48 hours. Proceeding incubation, 3 colonies were aseptically removed from each plate and placed into an individual glass culture tube containing 5 mL of NZY+ broth and 5 μL of AMP (100mg/mL solution). These culture tubes were incubated overnight at 37 °C in a rotating shaker.

Mutant plasmids were prepared and purified for sequencing with a Wizard Miniprep DNA Purification System. Broth culture tubes were taken from the rotating incubator and 1.5 mL- Eppendorf microcentrifuge tubes were labeled to match one of the culture tubes. 1.5mL of the cell mixture was removed from the broth culture tubes via pipette and placed into the correspondingly labeled Eppendorf tubes using aseptic techniques. Each tube was centrifuged for one minute in a microcentrifuge at 10,000 rpm. Afterwards, the resulting supernatant was poured off and more cell mixture was added. This procedure was followed until all of the cell mixture was pelleted. Supernatant was again poured off, but the remaining broth was removed with a pipettor. 400 µL of cell resuspension solution was introduced to the pellet, and pipetted up and down until all of the cells were off of the wall and resuspended. 400 µL of lysis solution was added and mixed by 4 gentle inversions of the tube. The suspension immediately cleared and 400 µL of Neutralization solution was added. Again, a gentle mixing was achieved by four inversions, as vortexing the cell solution would have caused shearing of the DNA. The cell lysate was centrifuged at 10,000 rpm for 5 minutes, but it was crucial that a pellet formed or this step would have been repeated until a pellet formed. Supernatant was transferred to a 2.5-mL screw-cap Falcon tube with 1 mL of resin and mixed by inversion, followed by standing for 5 minutes. 5 mL syringes were prepared by removing the plungers, attaching a minicolumn, and transferring the resin and lysate mixture in. The mixture was pushed through the minicolumn and 2 mL of column wash was then added to again push through the minicolumn. The minicolumn was removed from the syringe and placed on an Eppendorf microcentrifuge tube, and then centrifuged at 10,000 rpm for 2 minutes to dry the resin. The minicolumn was transferred to a new Eppendorf microcentrifuge tube, where 50 µL of preheated 70 °C sterile H_2O directly on the

resin, and allowed to sit for one minute. This was centrifuged at 10,000 rpm for 1 minute, the flow through from the column now in the Eppendorf tube was labeled and stored at -80 °C.

To make sure that the prepared plasmids contained the selected mutations, they were sent to the DNA Sequencing Laboratory at the University of Arkansas for sequencing. These samples for sequencing were prepared from the plasmid preparations. 495 µL of sterile ddiH_2O and 5 µL of the plasmid preparation, a 1:00 dilution, were placed in a quartz cuvette and the concentration of the plasmid was calculated from absorbance measurements. 500 ng of plasmid per sample was desired, and so the volume of plasmid needed was calculated. 2.9 µL of the sequencing primer and plasmid were added to a labeled, sterile 1.5-mL Eppendorf tube along with enough sterile ddiH_2O to reach a volume of 13 µL. Results from sequencing validated that the plasmids did uptake the desired mutations.

Transformation with Mutant Plasmid

The Y97E-only mutant Cyt *c* plasmid was needed to transform *E. coli* BL21-DE3 competent cells. 6 liters of Terrific Broth was prepared and autoclaved. The desired plasmid and E.Coli stock from the -80°C freezer were kept on ice until thawed. A Falcon screw-cap tube was pre-chilled and 2 µL of the plasmid and 25 µL of *E. coli* competent cells were added. The suspension was gently mixed by pipetting then allowed to incubate on ice for 30 minutes, followed by 2 minutes of heat-pulsing at 42 °C and then returned to ice for 2 minutes. After 500 µL of 2xYT broth were added, the mixture was placed in a 37 °C incubator for 1 hour. The mixture was spread plated onto a 2xYT+AMP agar plate with a overnight incubation. With sterile toothpicks, a colony was aseptically removed from the plate and dropped into a 6L Erlenmeyer flasks containing 2 L of sterile Terrific broth with 2mL of AMP, three toothpicks dropped in each flask. These flasks were placed on orbital shakers and incubated at 37 °C for 48 hours.

Cytochrome c Purification

After incubation, harvesting was achieved by centrifuging the cell suspensions in 500 mL pre-weighed centrifuge bottles in a JA-10 rotor of a Beckman-Coulter Avanti J-A preparatory centrifuge at 10,000 rpm for 15 minutes. The resulting supernatant was discarded. 3 mL of lysis buffer, containing of 50 mM Tris pH 8, 5 mM EDTA, 10 mM magnesium sulfate, and 1 mM calcium chloride, per gram cell paste was added to the cell paste. 9 mg of lysozyme was added per gram of paste, as was 32 µL per gram pellet of 50 mM PMSF in ethanol (phenylmethylsulfonyl fluoride). After stirring in room temperature for 20 minutes, a few crystals of DNase were added and the mixture was moved to a 37 °C incubator to stir for 20 more minutes. Then the mixture was removed from the incubator and followed by 1 hour of stirring in room temperature. The mixture was placed in a freezer-proof container to be stored overnight at -80 °C. The mixture was then thawed and centrifuged at 18,000 rpm and 4 °C for 30 minutes, keeping the supernatant. While stirring on ice, ammonium sulfate was added to bring the cell lysate to a concentration of 50% saturation. After the mixture mixed for 30 minutes it was centrifuged at 18,000 rpm to remove large particles. Supernatant was poured off again and ammonium sulfate was added to a concentration of 90% saturation at 4 °C. After mixing for 30 minutes on ice, this was centrifuged again, but the resulting pellet was kept and the supernatant was discarded. The pellet was resuspended with enough water to reintroduce it back into solution. Following was an overnight dialysis with a 6,000 – 8,000 MWCO against 5 L of 10mM Tris pH 8.0 at 4°C, with one complete buffer change after 4-6 hours. Dialysate was centrifuged to remove any precipitate, and then loaded onto a Sephadex S-Sepharose cation-exchange chromatography column, which was equilibrated with 50 mM Tris, pH 8. A gradient maker was set up with

high and low salt solutions- 50 mM Tris, pH 8, with 500 mM sodium chloride as high and 50 mM Tris, pH 8, as the low salt solution. Fractions were collected every two minutes using a fraction collector. Those fractions with red color, characteristic of Cyt *c*, were taken to the spectrophotometer for absorbance readings- 280 nm (for protein concentration) and 410 nm (for the heme group of Cyt *c*).

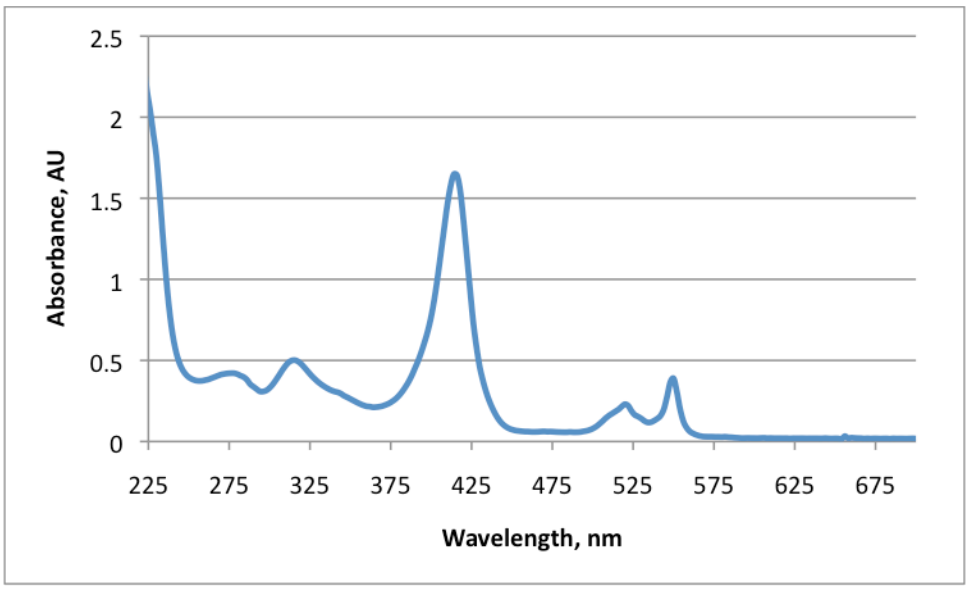

Figure 4: Example of a characteristic Cyt *c* absorbance spectrum. Characteristic peaks for Cyt *c* at 416 and 550 nm.

Fractions with an absorbance reading higher at 410 nm than the readings at 280 nm were combined and concentrated to a final volume of 15 mL by placing into a 10,000 MWCO concentrator at 4,000 rpm, exchanged with 5 mM sodium phosphate (P*i*), pH 7.0, to reduce the salt concentration and the conductivity of the solution.

High-pressure liquid chromatography (HPLC) was the final step in purification. On a Hitachi LaChrom Elite HPLC system, buffer reservoirs were degassed, Cyt *c* was oxidized

with a small amount of potassium ferricyanide ($K_3Fe(CN)_6$), and loaded onto the BioRad UNO S12 cation exchange column.

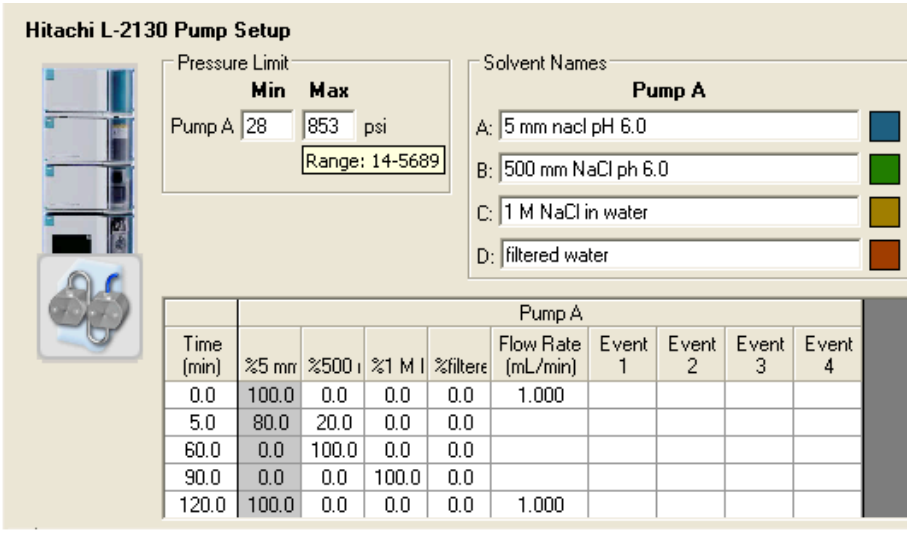

Figure 5: Example of an HPLC gradient for purification of Cyt *c*.

The diode array detector was set to monitor absorbance at 280 nm, 410 nm, and 542 nm, with fractions collected by an automated fraction collector. Fractions containing Cyt *c* were again combined and concentrated in a 10,000 MWCO concentrator at 6,000 rpm. These were divided into 100 µL aliquots and frozen at -80 °C.

Cytochrome c Oxidase Purification

Purified bovine CcO had previously been prepared in the lab by the same procedure described by Capaldi (12).Small aliquots were stored in the -80 °C freezer and a single aliquot of CcO was removed from the freezer and thawed on ice for each experiment.

Analytical Ultracentrifugation

The dissociation constant (K_d) for the binding between Cyt *c* and CcO was analyzed using analytical ultracentrifugation techniques. Ultracentrifugation takes advantage of sedimentation coefficients; large proteins or protein complexes have larger sedimentation coefficients than small proteins, thus they move outward rapidly. CcO is a much larger protein than Cyt *c*, which results in an even larger complex size when bound together. CcO and the Cyt *c*-CcO complex sediment more rapidly during ultracentriguation than unbound Cyt *c*, and therefore Cyt *c* remains in solution is separated. This separation allows for the concentration of unbound Cyt *c* in the sample to be measured over several time points to calculate K_d.

Experiments with both wild type and Y97E mutant Cyt *c* were completed. The experiments involved a salt titration, in which several ultracentrifuge runs were performed. The initial sample cells contained no salt, and were therefore at low ionic strength, while the final cells were at high salt and ionic strength where Cyt *c* would not bind to CcO.

The CcO concentration within the ultracentrifuge sample cell was approximately 7 μM and the concentration of Cyt *c* was lower, approximately 5 μM, so that CcO was in excess. The excess CcO permitted that all of the Cyt *c* to be bound to CcO at zero salt.

Samples were prepared by exchanging CcO with 5 mM P*i*, pH 7.4, with 0.2% lauryl maltoside, and the concentration of CcO was measured with absorbance readings at 420 – 460 with an extinction coefficient of 134 mM^{-1} or 598 minus 630 nm with an extinction coefficient of 12.7 mM^{-1}. Cyt *c* was added by a similar technique, as the concentration was also determined spectrophotometrically from absorbance at 410 nm. The ultracentrifuge cell contained 300 μL of the prepared sample. Each ultracentrifuge run was approximately 1 hour and 15 minutes, at 48,000 rpm and 22 °C. Using a monochromator head, absorbance scans were taken every 10 minutes at 410 nm. The salt concentration within the cell was increased after each run by adding 2 or 5 M NaCl. The salt concentrations for the ultracentrifuge runs were 0, 50, 100, 150, 200, and 350 mM. The concentrations of the last runs were high-salt concentrations, with a goal to inhibit nearly all binding of Cyt *c* to CcO. The resulting data was analyzed to determine the K_d value for the protein complex containing wild-type Cyt *c* or mutant Y97E at each salt concentration.

Flash Photolysis – Reduction of Ruthenium-39- Cyt *c*

Electron transfer with Cyt *c* was studied using a previously prepared Ru-39 Horse Cyt *c,* which has the ruthenium complex ($Ru(bpy)_2(mobpy)$) covalently bound to horse Cyt *c* at a constructed Cys-39. The inhibition of electron transfer rate from Ru-horse Cyt *c* to bovine CcO was studied by addition of human Cyt *c*, both wild type and mutant Y97E.

The covalent attachment of the ruthenium complex was prepared by the same methods as described by Geren (*15*). The sacrificial donors for the ruthenium complex were aniline and 3CP. Ionic strength was increased with 5mM phosphate buffer (Pi) pH 7.0 in 0.1% LM, by addition of 2M NaCl. Excess salt was removed from CcO with an Amicon concentrator with a molecular weight cut off of 100,000 daltons. Reaction solutions contained 5.0 μM bovine CcO, 10 μM Ru-39- Cyt *c*, 5mM phosphate buffer pH 7.0 in 0.1% lauryl maltoside, 1mM 3CP, 10mM aniline, and varying concentrations of human Cyt *c*. Separate experiments were conducted for native or mutant Cyt *c*. The total sample volume was consistently 300 μL, contained in a 1cm glass or quartz cuvette.

The concentrations of Ru-39- Cyt *c*, native or mutant Cyt *c*, and bovine CcO were found using a Hewlett Packard 8452A diode array spectrometer with a UV filter. Flash photolysis experiments were conducted as described by Geren et al. (*15*). Blanks were taken at 600 and 550 nm. The ruthenium was excited with a Phase R model DL1400 flash lamp-pumped dye laser producing a 450nm light pulse with <0.5μs duration. Absorbance transients were recorded at 600 and 550 nm, using appropriate time scales.

Nine trials were conducted for both wild type and mutant Y97E. 10 μM wildtype or mutant human Cyt *c* were added to the sample after the first trial, and the third trial contained

an additional 10 μM Human Cyt *c* for a total of 20 μM Human Cyt *c*. The fourth trial began the salt titrations- increasing the concentration throughout the experiment: 50, 90, 150, 170, 200, and 350 mM NaCl.

After the experiment was completed, Na dithionite was used to reduce the sample for final concentration measurements. The equations 2 and 3 were used to calculate the final concentration of the ruthenium derivative, native horse Cyt *c*, native human Cyt *c*, and bovine CcO.

Equation 2: $[\text{Cyt } c] = (A_{550} - A_{442})/ 17.8$

Equation 3: $[\text{CcO}] = (A_{605} - A_{630})/33$

The absorbance transients were fitted using the SI fittings program written by Tracy Jackson. A 600 nm filter with a 10 nm bandwidth was used to measure the reduction of heme a, the extinction coefficient used was $\Delta\varepsilon_{604} = 16\ mM^{-1}\ cm^{-1}$ (*16*).

Results and Discussion

Analytical Ultracentrifugation

The analytical ultracentrifuge took absorbance scans taken every 10 minutes at 410 nm at varying radii within the cell. The absorbance data for wild-type Cyt *c* and the Y97E Cyt *c* can be seen in figures 6 and 7. Data from trials with different salt concentration were complied onto a single graph, and the salt concentrations were labeled by color. Each graph contained a spike in absorbance at approximately 6.35 cm, which represents the meniscus of the fluid in the sample cell. Data points plateau at approximately 6.5 cm.

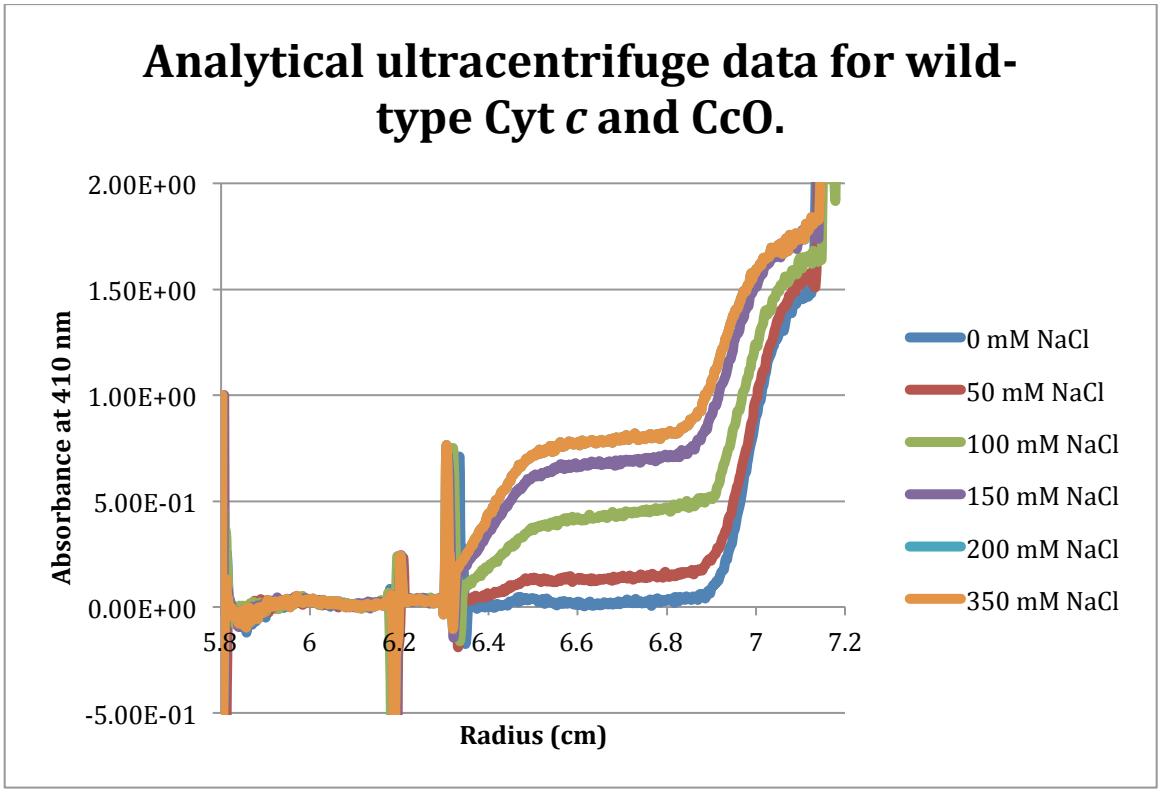

Figure 6: Analytical ultracentrifuge data for wild-type Cyt *c* and CcO.

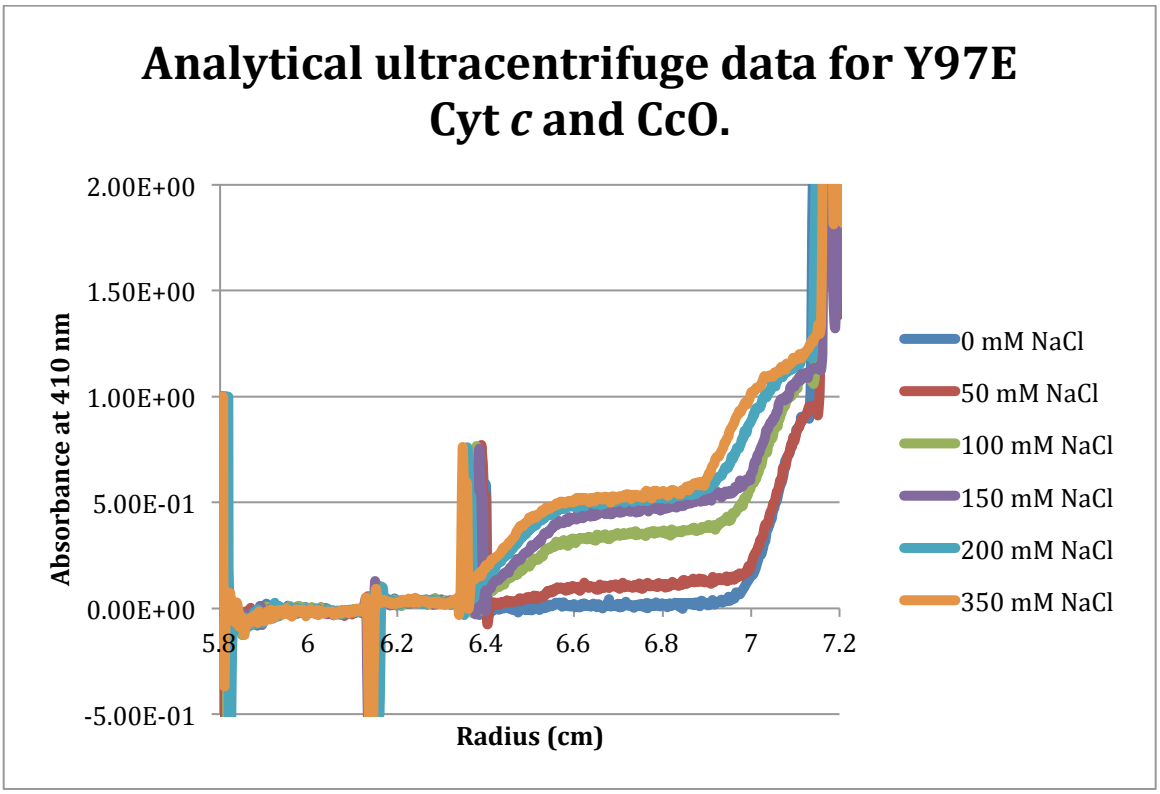

Figure 7: Analytical ultracentrifuge data for Y97E Cyt *c* and CcO.

The concentration of free Cyt *c* was calculated by the absorbance at the plateau and the absorbance at the baseline radius using Beer's law. The extinction coefficient was 106 mM^{-1} cm^{-1}. Calculations for bound Cyt *c* required the subtraction of the concentration of free Cyt *c* from the initial concentration of Cyt *c* within the sample. The concentration of bound CcO was equal to the concentration of bound Cyt *c* because there is 1:1 binding relationship. Free CcO within the solution was calculated by subtracting the concentration of bound CcO from the original CcO concentration. Determination of the K_d value for each ultracentrifuge run could then be solved for using equation 4. Error limits were ± 20 %.

Equation 4: $K_d = \frac{([\text{Cyt } c]_{free} * [\text{CcO}]_{free})}{[\text{Cyt } c\text{*CcO}]_{bound}}$

Equation 5: $[\text{Cyt } c]_{Total} = [\text{Cyt } c]_{free} + [\text{Cc*CcO}]_{bound}$

Equation 6: $[\text{Cyt } c\text{*CcO}]_{bound} = [\text{Cyt } c]_{Total} - [\text{Cyt } c]_{free}$

Equation 7: $[\text{CcO}]_{Total} = [\text{CcO}]_{free} + [\text{Cyt } c\text{*CcO}]_{bound}$

Equation 8: $[\text{CcO}]_{free} = [\text{CcO}]_{Total} - [\text{Cyt } c\text{*CcO}]_{bound}$

Results of these calculations for each experiment are shown in Table 3.

[NaCl] mM	**K_d for WT Cyt *c* (μM)**	**K_d for Y97E Cyt *c* (μM)**
0	<0.2	<0.2
50	0.5 ± 0.1	0.5 ± 0.1
100	5.6 ± 1.1	6.1 ± 1.2
150	31.7 ± 6.3	20.5 ± 4.1
200	>40	>40
350	>40	>40

Table 3: K_d values determined from analytical ultracentrifuge experiments.

Larger values for K_d indicate that higher concentrations of free protein and lower concentrations of bound protein were present in the sample cell. A significant difference in K_d value would suggest that the Cyt *c* of higher K_d value binds less tightly to CcO than the Cyt *c* with a lower K_d value.

K_d values of wild-type Cyt *c* and the Y97E Cyt *c* were found to be very similar upon comparison, suggesting that phosphorylation at the Y97 residue does not affect binding between Cyt *c* and CcO.

Flash Photolysis – Reduction of Ruthenium-39- Cyt *c*

The electron transfer within the Cyt *c* -CcO complex was measured utilizing a photoactive tris(bipyridine)ruthenium group (Ru(II)) covalently attached to horse Cyt *c* at position 39 (Ru-39- Cyt c). Ru (II) was photoexcited by a laser, inciting a rapid electron transfer to the heme in Ru-39-Cyt c. The photo-reduced heme subsequently transferred an electron to the Cu_A in CcO, followed by a transfer to heme a. Rate constants were determined by changes of absorbance measurements; increased absorbance at 600 nm is seen when an electron is transferred from Cu_A to heme a. Next, the electron traveled to Cu_B and a decrease in absorbance is seen at 600 nm due to the oxidation of heme a *(13)*.

Human Cyt *c* and the Ruthenium-39-Cyt *c* compete for the binding site on CcO. Salt weakens complex binding so that it dissociates. At low salt, electron transfer from the heme of Cyt *c* to Cu_A in CcO is observed as the fast phase. An internal electron transfer within CcO then occurs - Cu_A to heme a. The Cyt *c*-CcO complex dissociates in the slow phase, seen at high salt. A scheme of the electron transfer is shown in Figure 8.

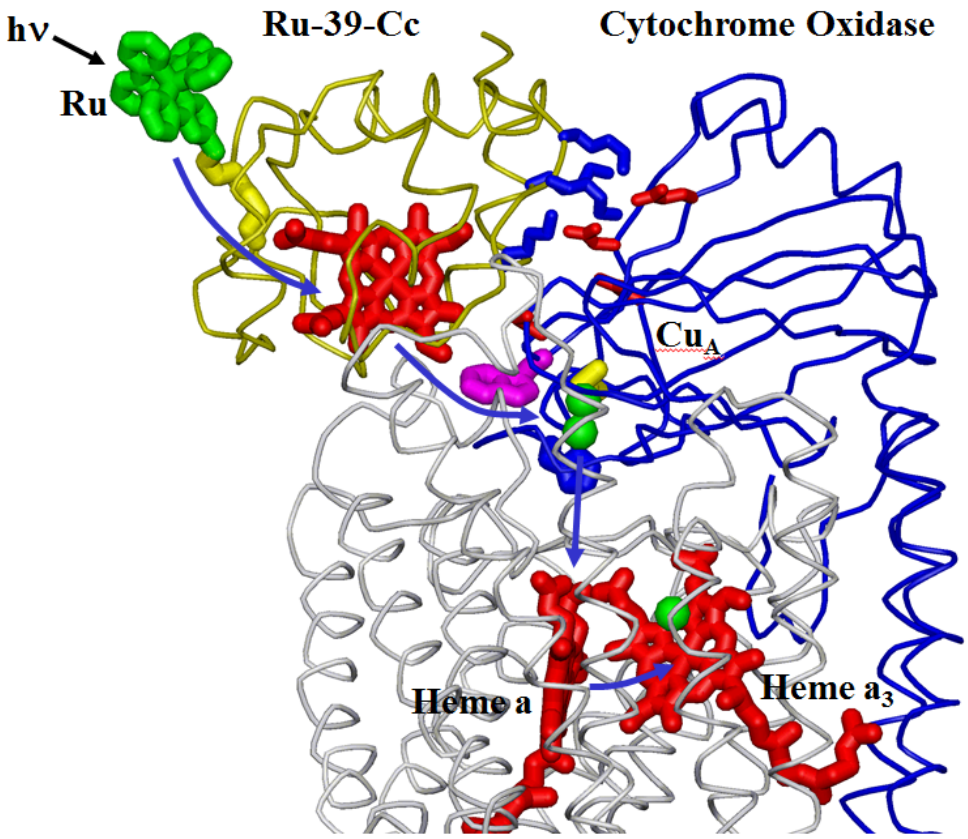

Figure 8: Ru-39- Cyt *c*. The laser light strikes Ru. Excitation of Ru results in electron transfer, seen by the blue arrows *(14)*.

$$Cyt\ c_{human} + CcO \underset{K_d}{\overset{K_f}{\rightleftharpoons}} Cyt\ c_{human} - CcO$$

$$Ru - 39 - Cyt\ c + CcO \underset{K_d}{\overset{K_f}{\rightleftharpoons}} Ru - 39 - Cyt\ c - CcO$$

Equation 9: Binding of human Cyt c to CcO
Equation 10: Binding of Ru-39-Cyt c to CcO.

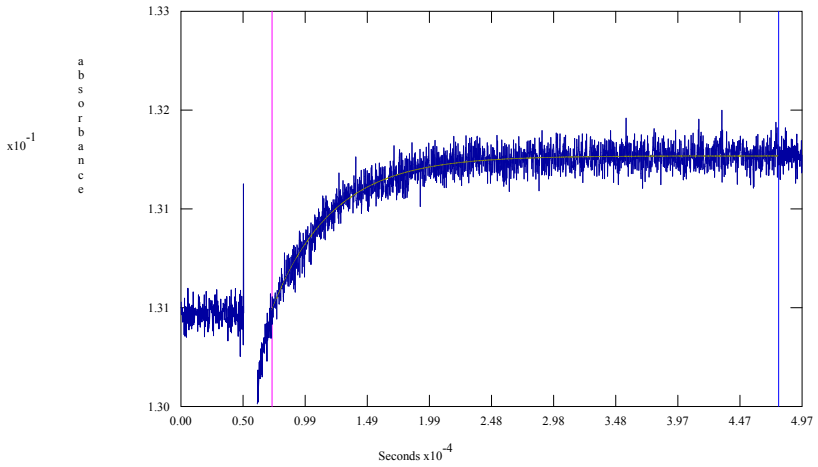

Figure 9: 5.60uM Bovine CcO. 10.16uM Ru-39-Cyt c. Aniline 10mM. 3CP 1mM. 600nm.

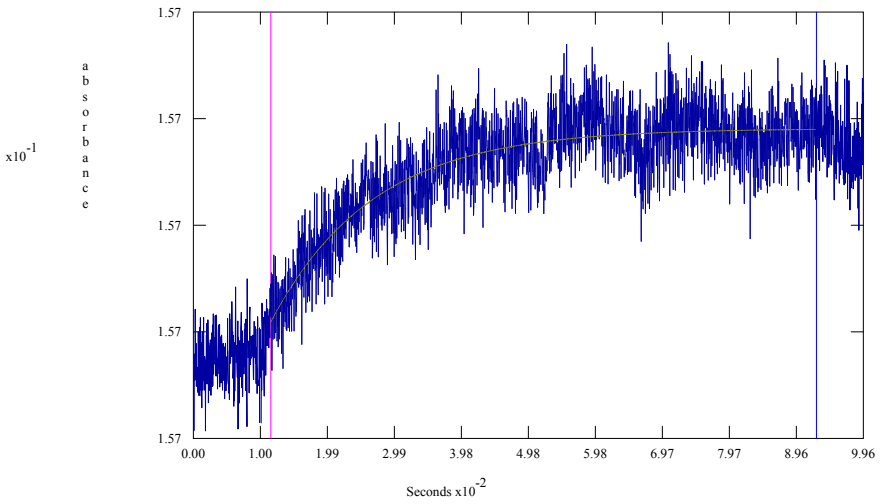

Figure 10: 5.60uM Bovine CcO. 10.16uM Ru-39-Cyt c. Aniline 10mM. 3CP 1mM. 600nm. 9.9uM Human WT-Cyt c.

Flash photolysis absorbencies are measured at 550 and 600 nm; measuring electron transfer to Cyt *c* at 550nm and electron transfer to CcO heme a measured at 600nm. Rate constants at varying ionic strengths were commuted via a computer system.

[NaCl] mM	0	50	90	150	170	200
WT rate (1/s)	52± 10	96± 19	274± 55	322± 64	318± 64	257± 51
Y97E rate (1/s)	74± 15	88± 18	254± 51	382± 76	316± 63	200± 40

Table 4: Electron transfer rates with increasing [NaCl]. Flash photolysis, 600 nm transients, 5.60 uM Ru horse Cyt Cyt *c*, 20.1 uM WT, 21.2 uM Y97E.

Electron transfer rates of WT human Cyt *c* were compared to human Y97E. Comparison of electron transfer rates between wild-type Cyt *c* and Y97E Cyt *c* were very similar, and once again led to the conclusion that phosphorylation at the Y97 residue does not affect binding between Cyt *c* and CcO.

Conclusions

The phosphomimetic mutant of Cyt *c* was well expressed. There was no significant difference in the binding of WT and mutant Y97E Cyt *c* to CcO. The results of the ruthenium kinetics studies are in Table 4. The electron transfer rate constants are proportional to the rate constant of dissociation of the complex between Cyt *c* and CcO. There was no significant difference in the rate constant of dissociation for wild-type and mutant Y97E Cyt *c* from CcO. In conclusion, preliminary studies on the effect of the phosphomimetic mutation of Cyt *c* on the electron transfer reaction between Cyt *c* and CcO have indicated that the Y97E mutation does not have an effect on the Km of the reaction or electron transfer rate.

References

1. Pecina, P., Borisenko, G. G., Belikova, N. A., Tyurina, Y. Y., Pecinova, A., Lee, I., Samhan-Arias, A. K., Przyklenk, K., Kagan, V. E., and Hüttemann, M. (2010) Phosphomimetic Substitution of Cytochrome cTyrosine 48 Decreases Respiration and Binding to Cardiolipin and Abolishes Ability to Trigger Downstream Caspase Activation. *Biochemistry* **49**, 6705–6714
2. Hüttemann, M., Helling, S., Sanderson, T. H., Sinkler, C., Samavati, L., Mahapatra, G., Varughese, A., Lu, G., Liu, J., Ramzan, R., Vogt, S., Grossman, L. I., Doan, J. W., Marcus, K., and Lee, I. (2012) Regulation of mitochondrial respiration and apoptosis through cell signaling: Cytochrome c oxidase and cytochrome c in ischemia/reperfusion injury and inflammation. *BBA - Bioenergetics* **1817**, 598–609
3. Morriss, G. M., and New, D. A. (1979) Effect of Oxygen concentration on morphogenesis of cranial neural folds and neural crest in cultured rat embryos, *J. Embryol. Exp. Morphol. 54,* 17- 35.
4. Yu, H., Lee, I., Salomon, A. R., Yu, K., and Hüttemann, M. (2008) Mammalian liver cytochrome c is tyrosine-48 phosphorylated in vivo, inhibiting mitochondrial respiration. *Biochimica et Biophysica Acta (BBA) - Bioenergetics* **1777**, 1066–1071
5. Li,K., Li, Y., Shelton, J. M., RRichardson, J.A., Spncer, E., Chen, Z. J., Wang, X., and Williams, R. S. (2000) Cytochrome *c* deficiency causes embryotic lethalityand attenuates stress-induced apoptosis. Cell 101, 389-399.
6. Kadenbach, Bernhard, Rabia Ramzan, and Sebastian Vogt. "Degenerative Diseases, Oxidative Stress and Cytochrome C Oxidase Function." *Trends in Molecular Medicine* 15.4 (2009): 139-47.
7. Sanderson, T. H., Reynolds, C. A., Kumar, R., Przyklenk, K., and Hüttemann, M. (2012) Molecular Mechanisms of Ischemia–Reperfusion Injury in Brain: Pivotal Role of the Mitochondrial Membrane Potential in Reactive Oxygen Species Generation. *Mol Neurobiol* **47**, 9–23
8. Hüttemann, M., Lee, I., Grossman, L. I., Doan, J. W., and Sanderson, T. H. (2012) Phosphorylation of mammalian cytochrome c and cytochrome c oxidase in the regulation of cell destiny: respiration, apoptosis, and human disease. *Adv. Exp. Med. Biol.* **748**, 237–264
9. Bender, E., and Kadenbach, B. (2000) The allosteric ATP-inhibition of cytochrome c oxidase activity is reversibly switched on by cAMP-dependent phosphorylation. *FEBS Lett.* **466**, 130–134
10. Millett, F., and Durham, B. (2002) Design of Photoactive Ruthenium Complexes To Study Interprotein Electron Transfer †. *Biochemistry* **41**, 11315–11324
11. Durham, B., and Millett, F. (2012) Design of photoactive ruthenium complexes to study electron transfer and proton pumping in cytochrome oxidase. *Biochim. Biophys. Acta* **1817**, 567–574
12. Capaldi, R. A., and Hayashi, H. (1972) The Polypeptide Composition of Cytochrome Oxidase from Beef Heart Mitochondria, *FEBS LETTERS 26*, 261-263.

13. Zaslavsky, Sadoski, Rajagukguk, Geren, Millett, Durham, and Gennis. Direct measurement of proton release by cytochrome c oxidase in solution during the F→O transition. *PNAS*, July 20, 2004, vol 101, no. 29, 10544-10547
14. Gennis R., Ferguson-Miller S., Structure of Cytochrome c Oxidase, Energy Generator of Aerobic Life. *Science*, Vol. 269, 25 August 1995 pp 1063-1064
15. Geren, L., Hahm, S., Durham, B., and Millett, F. (1991) Photoinduced Electron Transfer between Cytochrome c Peroxidase and Yeast Cytochrome c Labeled at Cys 102 with (4-Bromomethyl-4'-methylbipyridine)[bis(bipyridine)]ruthenium^{2+}, *Biochemistry 30*, 9450-9457.
16. Blair, D. F., Bocian, D. F., Babcock, G. T., and Chan, S. I. (1982) Evidence for Modulation of the Heme Absorptions of Cytochrome c Oxidase by Metal-Metal Interactions, *Biochemistry 21*, 6928-6935.
17. Liu, X., Kim, C. N., Yang, J., Jemmerson, R., and Wang, X. (1996) Induction of apoptotic program in cell-free extracts: requirement for dATP and cytochrome c. *Cell* **86**, 147–157
18. García-Heredia, J. M., Díaz-Quintana, A., Salzano, M., Orzáez, M., Pérez-Payá, E., Teixeira, M., Rosa, M. A., and Díaz-Moreno, I. (2011) Tyrosine phosphorylation turns alkaline transition into a biologically relevant process and makes human cytochrome c behave as an anti-apoptotic switch. *J. Biol. Inorg. Chem.* **16**, 1155–1168